Reaction Chemistry & Engineering

ROYAL SOCIETY OF CHEMISTRY

PAPER

View Article Online
View Journal | View Issue

Cite this: *React. Chem. Eng.*, 2026, 11, 367

A technology for whole-component utilization of refractory ferromanganese ores: hydrogen-based mineral phase transformation

Jiali Chen,[abc] Peng Gao,[abc] Jie Liu,[abc] Yimin Zhu[abc] and Wentao Zhou *[d]

Received 18th September 2025,
Accepted 17th October 2025

DOI: 10.1039/d5re00418g

rsc.li/reaction-engineering

To address the low utilization rate of refractory ferromanganese ores, this study proposes an innovative technology, namely the pre-enrichment-hydrogen-based mineral phase transformation–magnetic separation, to realize the separation and enrichment of manganese and iron from the ores. The suitable process parameters were determined as follows: a pre-enrichment magnetic field strength of 6500 Oe, a processing capacity of 80 kg h^{-1}, a CO dosage of 7.5 m^3 h^{-1}, a H_2 dosage of 3.8 m^3 h^{-1}, a N_2 dosage of 13.8 m^3 h^{-1}, a roasting temperature of 500 °C, a total gas volume of 25.1 m^3 h^{-1}, an excess coefficient of the reductant of 1.4, and a magnetic field strength of 1520 Oe. Through the stabilization test, iron concentrate with a TFe grade over 67% and iron recovery over 87% and manganese concentrate with manganese grade over 48% and manganese recovery rate over 77% can be obtained. Product analysis reveals that pre-enrichment technology achieved the removal of silicon containing gangue minerals, and the iron-containing minerals (mainly hematite) and manganese-containing minerals (pyrolusite, braunite, psilomelane, and manganite) are selectively converted to magnetite and manganosite, respectively, through mineral phase transformation. The magnetite and manganosite are then cleanly and efficiently separated and enriched in the magnetic concentrate and tailings, respectively, by weak magnetic separation.

1 Introduction

Iron and manganese are two of the basic bulk raw materials necessary for industrial production. China is the largest consumer and importer of iron and manganese resources in the world, and its dependence on foreign countries for iron and manganese ore resources exceeds 80%, which has become a major hidden danger for the stable operation of China's economy and the healthy development of the society. China and its overseas rights and interests together hold more than 280 million tons of retained manganese resource reserves. Because refractory ferromanganese ores have complex mineral compositions, similar physical and chemical properties, and finely embedded particle sizes, conventional beneficiation technology cannot achieve satisfactory technical or economic indexes. Therefore, developing independent innovative technologies to realize the efficient and comprehensive utilization of refractory ferromanganese ore resources is of great strategic significance for enhancing China's ferromanganese resource security.[1–4]

At present, the methods of treating refractory ferromanganese ore resources mainly include physical, chemical, and biological methods.[5–11] Tripathy *et al.*[12] carried out a test study on the gravity concentration of ferromanganese ore (22.42%Mn, 14.46%Fe) by using an interfering-bed separator (Floatex density separator) and obtained a better separation index. Zhang *et al.*[13] carried out an experimental study for a ferromanganese polymetallic ore (18.05% Mn, 14.65% TFe) in Xinjiang by using a weak magnetic separation and strong magnetic separation process. The results showed that under the optimized conditions of a grinding fineness of −0.074 mm (85.70%), a weak magnetic separation field strength of 0.08 T, and a strong magnetic separation field strength of 0.60 T, an iron ore concentrate with an Fe grade of 63.52% and an Fe recovery of 54.66% and a manganese ore concentrate with a Mn grade of 31.25% and a Mn recovery of 65.44% were obtained. You *et al.*[14] conducted an experimental study on sulfidation roasting–water leaching for a Mn ore containing Fe (14.30% Mn, 30.35% Fe) in Jiangxi. The results showed that the leaching temperature and time played a key role, and with the increase in leaching temperature, the dissolution rate of sulfate was accelerated and the extraction rate increased.

[a] *State Key Laboratory of Mineral Processing, Northeastern University, Shenyang 110819, China. E-mail: neuchenjiali@163.com, gaopeng__neu@163.com, liujie__neu@163.com, zhuyimin__neu@163.com*
[b] *School of Resources and Civil Engineering, Northeastern University, Shenyang 110819, China*
[c] *National-local Joint Engineering Research Center of High-efficient Exploitation Technology for Refractory Iron Ore Resources, Shenyang 110819, China*
[d] *College of Energy and Mining Engineering, Shandong University of Science and Technology, Qingdao 266590, P.R. China. E-mail: zhouwentao@sdust.edu.cn*

Table 1 Chemical multi-element analysis results/%

Component	TFe	FeO	Mn	Mn^{2+}	SiO_2	Al_2O_3
Content	44.71	<0.1	17.86	<0.1	5.08	1.98
Component	CaO	MgO	P	S	LOI	—
Content	0.18	0.26	0.022	0.004	2.72	—

Wang *et al.*[15] conducted an experimental study on an iron-containing manganese ore (13.28%Mn, 6.19%Fe) in Sichuan by using an acidophilic ferrous-oxidizing *Thiobacillus* bioleaching method. The results showed that the produced biological Fe^{3+}, H^+, and extracellular polymeric substances significantly contributed to metal recovery and effectively reduced the H_2S emission in the exhaust gas. Meanwhile, the radical and non-radical reactions occurring during the advanced oxidation process triggered the generation of a large number of reactive substances, while the charge transfer process contributed to the effective degradation of sulfathiazole (STZ). Under optimized conditions, a leach solution with metal leaching yields of 95.94% Mn and 97.54% Fe was obtained.

In summary, physical methods are characterized by relatively simple operation and low cost, but relatively poor results. Chemical leaching methods are characterized by high extraction rates and good selectivity but poor environmental friendliness. Bioleaching methods are environmentally friendly but characterized by long bacterial cultivation periods and low production efficiency. Hydrogen-based mineral phase transformation technology is one of the effective technologies for treating refractory ferromanganese ores and iron minerals.[16–20] Compared with traditional magnetization roasting technology, hydrogen-based mineral phase transformation technology has the advantages of efficient heat and mass transfer, uniform product quality, and low energy consumption. Previously, the author's team completed laboratory optimization tests and achieved excellent beneficiation results.[21–24] In this study, a pre-enrichment-hydrogen-based mineral phase transformation–magnetic separation technology to realize the clean and efficient separation and enrichment of manganese and iron in refractory ferromanganese ores from the perspective of testing is proposed.

2 Materials and methods

2.1 Raw material properties

2.1.1 Chemical composition analysis. The ferromanganese ore samples used in the tests were from Zambia. To determine the elemental composition of the sample, chemical multi-element analysis was conducted after crushing, mixing, and shrinking, and the results are shown in Table 1.

Table 1 indicates that the main metal elements in the ore samples are iron and manganese, with contents of 44.71% and 17.86%, respectively. The main impurity component is SiO_2 with a content of 5.08%. The contents of other impurities, Al_2O_3, CaO, and MgO, are 1.98%, 0.18%, and 0.26%, respectively, and the contents of phosphorus and sulfur are 0.022% and 0.004%, respectively.

2.1.2 Phase composition analysis. The chemical phase analysis method was used to analyze the iron and manganese phases of the sample by a chemical titration method, and the results are shown in Tables 2 and 3, respectively.

Tables 2 and 3 reveal that iron in the ore samples is mainly distributed in hematite with a distribution rate of 98.18%. The iron content in magnetic iron, iron carbonate, iron sulfide, and iron silicate is low, and their distribution rates account for 0.79%, 0.23%, 0.51%, and 0.28%, respectively. Manganese in the ore samples is mainly distributed in pyrolusite with a distribution rate of 77.35%. The second distribution is in braunite and manganite with a distribution rate of 18.83%. A small amount of manganese is distributed in rhodochrosite with a distribution rate of 3.82%.

2.1.3 Mineral composition analysis. The raw ore samples (−1 mm) were cured, smoothed, combined with optical microscope identification, X-ray diffraction (XRD), scanning electron microscopy–X-ray energy spectrometry analysis (SEM–EDS) and chemical multi-element analysis results, and the mineral composition and mineral content in the specimens were determined by using the process mineralogy automatic test system, and the results are listed in Table 4.

The results show that the iron minerals in the samples are mainly hematite (62.14%); manganese minerals are mainly pyrolusite (18.00%) and braunite (4.67%). The BSE images and BPMA mineral pseudo-color maps of the ore samples are shown in Fig. 1.

2.1.4 The embedding relationship of major minerals. The embedded relationship between the main minerals was analyzed by optical microscopy, and the results are shown in Fig. 2. Fig. 2 reveals that the embedded grain size of hematite in the mineral samples is coarse and mainly in the form of irregular grains. Most of the hematite in the specimen is richly congealed, often congealed with manganese oxides such as pyrolusite and psilomelane. The embedded grain size of pyrolusite in the sample is coarse mainly in the form of irregular granular aggregates, and often form iron-manganese oxide aggregates with hematite and hard manganese ores.

The hematite, pyrolusite, psilomelane, and braunite in the sample are closely interconnected and often form iron-

Table 2 Results of iron phase analysis (mass %)

Iron phase	Iron in hematite	Iron in magnetic iron	Iron in iron carbonate	Iron in iron sulfide	Iron in iron silicate	Total Fe
Content	42.04	0.34	0.1	0.22	0.12	42.82
Distribution rate	98.18	0.79	0.23	0.51	0.28	100.00

Table 3 Results of manganese phase analysis (mass %)

Manganese phase	Mn in rhodochrosite	Mn in braunite and manganite	Mn in pyrolusite	Total Mn
Content	0.69	3.40	13.97	18.06
Distribution rate	3.82	18.83	77.35	100.00

Table 4 Mineral composition and content of mineral samples

Mineral name	Content/%	Mineral name	Content/%
Hematite	62.14	Braunite	4.67
Pyrolusite	18.00	Quartz	2.96
Psilomelane	5.04	Barite	0.26

manganese oxide aggregates. The monomer content can reach 42.59%, and the content of rich connected organisms is 56.11%. The total content of richly connected organisms and monomers is 98.71%.

2.2 Equipment and methods

The test utilizes a continuous mineral phase transformation system. It mainly consists of the following systems: feeding system (including feed bin and loss-in-weight); mineral phase conversion system (including combustion station, mineral phase conversion furnace, cyclone separator, and fluidized reduction reactor); discharge system (including vertical cylinder cooler, reclaimer); dust collection system (including ceramic dust collector, ash chute, and bag filter); utility system (including Roots fan, gas system, CO gas system, N_2 system, water supply, and drainage system).

The material flow is as follows: the material is fed into the riser of the separating cyclone through the feeding bin, where the feeding quantity is controlled by the loss-in-weight weigher and feeding screw, and then it is fed into the riser of the separating cyclone. It is then preheated by the cyclone preheater and sent to the suspension roaster to heat up. Following this, it is reduced to obtain the reduction material in the magnetization reduction retention tank. Subsequently, it is sent to the riser cooler to cool down and then to the collector. The whole system adopts the negative-pressure operation, and the power is from the Roots blower. The exhaust gas is preliminarily de-dusted by a high-temperature dust collector and then enters the primary cooler; it is cooled to 160 °C and purified by a bag filter, and then it is cooled by a secondary cooler to less than 40 °C and discharged into the atmosphere by a fan. The dust from the high-temperature dust collector and bag filter enters the ash chute. The test process flow is as follows: when the main furnace of the mineral phase conversion furnace heats up to a predetermined temperature, start feeding the material at a certain rate, and when the reduction retention tank reaches a certain temperature, pass in N_2 and reduction gas according to a pre-set ratio to finally obtain the roasting product. Wet grinding of roasted ore samples is carried out using a laboratory rod mill (XMB-70) until all materials pass through a 100-mesh sieve and are then placed in a magnetic separation tube (XCGS) for weak magnetic separation, and the roasting effect was evaluated according to the magnetic separation results to determine the suitable

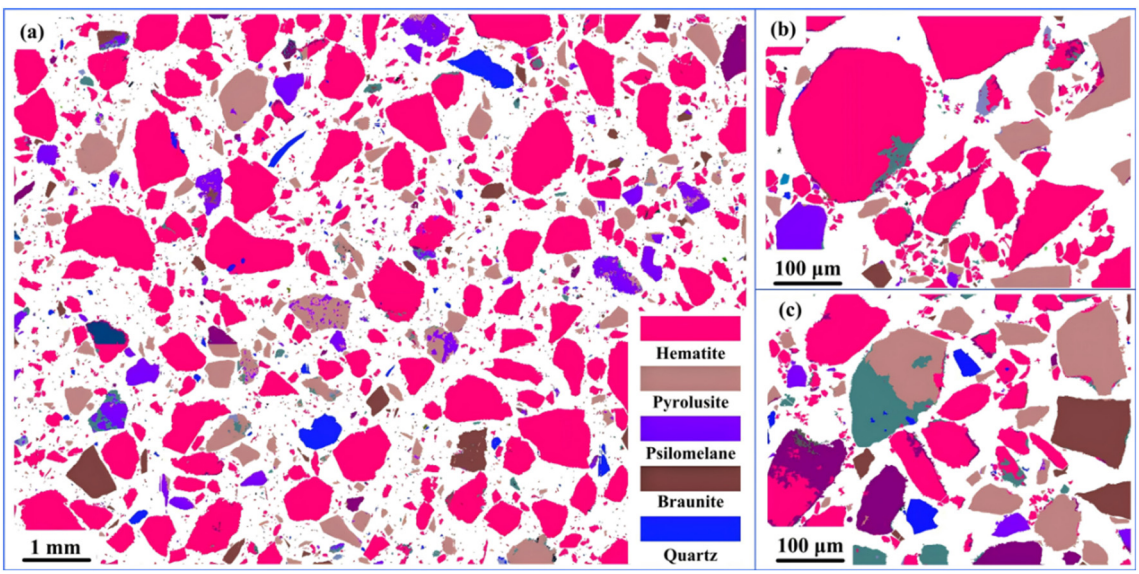

Fig. 1 (a) BSE images and BPMA mineral identification pseudo-color images of iron manganese ore samples; (b) fake color image of hematite; (c) pseudo-color image of pyroxene ore.

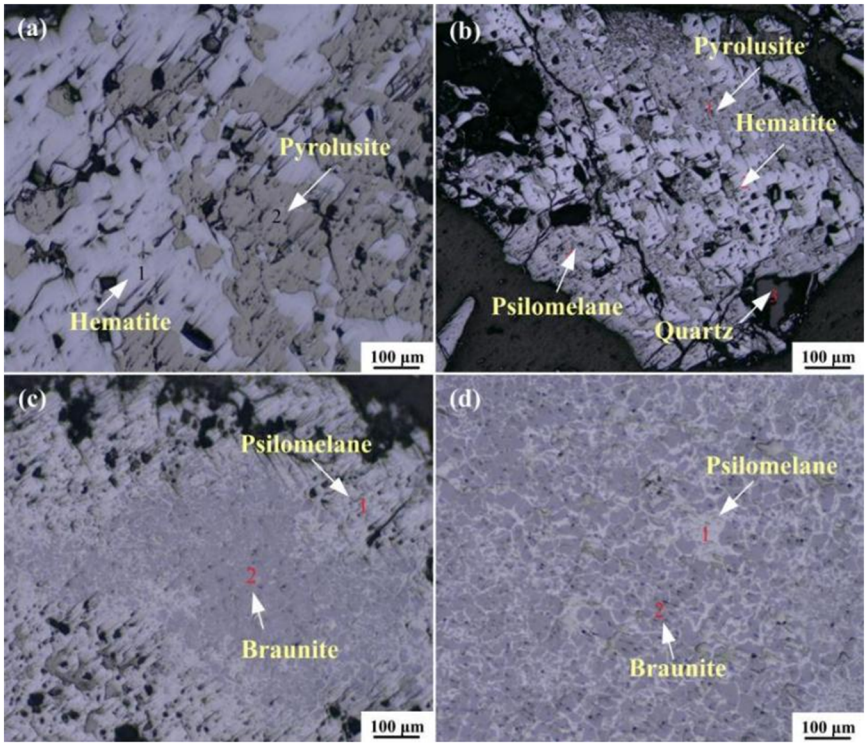

Fig. 2 Characteristics of the main minerals: (a) and (b) are pyrolusite closely associated with hematite and psilomelane; (c) and (d) are psilomelane closely associated with braunite, respectively.

conditions required for the stabilization test. After the condition test, a continuous stabilization test was carried out under suitable conditions. During the stabilization test, samples were taken every 1–2 h for 3–5 min each time, and the magnetic separation test was carried out, which was combined with the magnetic separation indexes to examine the smooth operation of the suspension roaster and the stability of the roasted product indexes. The process flowchart is shown in Fig. 3.

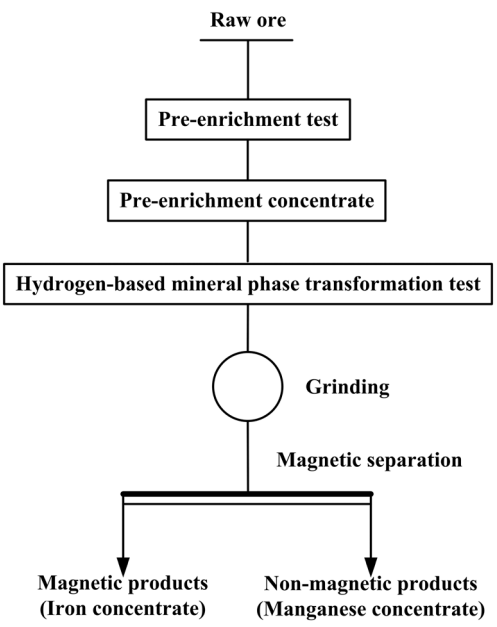

Fig. 3 The process flowchart.

In this study, XRD (D8 Advance X) was used to analyze the physical phase of the test products with the following operating parameters: operating voltage of 40 kV, operating current of 250 mA, scanning range of 10–70°, scanning rate of 10° min^{-1}. X-ray photoelectron spectroscopy (XPS, ESCALAB XI+, Al Kα, $h\upsilon$ = 1486.6 eV, full spectrum 160 eV, narrow spectrum 40 eV, resolution 0.05 eV) can be used to analyze the changes in the elemental composition of the surface of the samples before and after roasting and to detect the forms of their assignment. High-resolution transmission electron microscopy (HRTEM, JEOL JEM-2100PLUS, accelerating voltage 200 KV, ultrasonic time 10 min) was used to detect the lattice changes of the samples before and after roasting. Scanning electron microscopy (resolution 0.8 nm/15 kv, 1.6 nm/1 kv; accelerating voltage 20 V–30 kV; magnification 12–1 000 000 times) can observe the microscopic morphology of the samples, which has the advantages of a high magnification, clear images, and simple operation. Equipped with an X-ray spectrometer, it can qualitatively and quantitatively analyze the composition of the micro-region on the surface of the material while observing the micro-morphology. Field emission scanning electron microscopy (FESM) and energy dispersive spectroscopy (Apreo S HiVac) are used to characterize the micro-morphological structure and surface elements of the roasted samples.

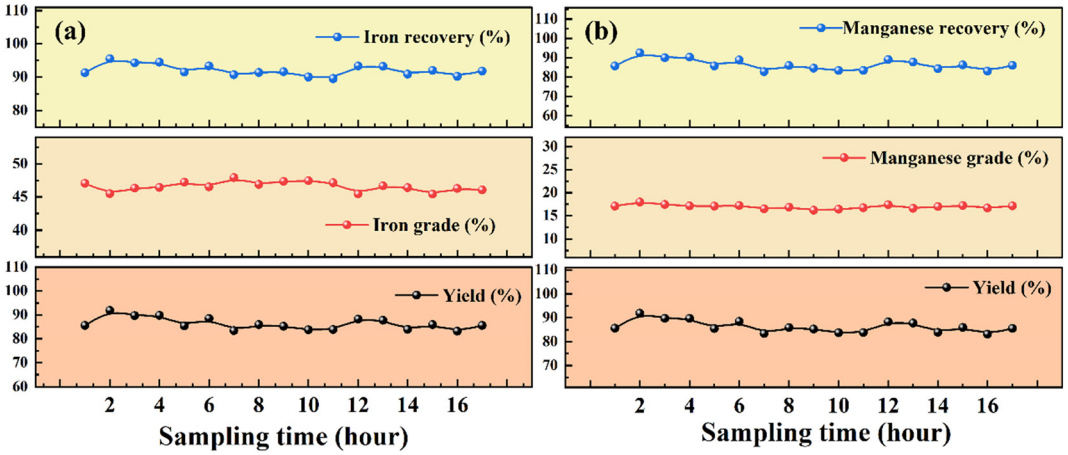

Fig. 4 Preparation experiment of pre-enriched concentrate: (a) yield, grade, and recovery of pre-enriched iron concentrate; (b) yield, grade, and recovery of pre-enriched manganese concentrate.

3 Results and discussion

3.1 Pre-enriched concentrate preparation test

Pre-enrichment of refractory ferromanganese ores can, on the one hand, effectively remove the sludge and part of the veinstone and reduce the influence of veinstone minerals and sludge on the subsequent suspension magnetization roasting operation. Meanwhile, it can obtain the pre-enriched crude concentrate material with suitable particle size and uniform quality and improve both the flow characteristics of the material in the phase transformation furnace and the cyclone separation effect of the material in the furnace. On the other hand, it can improve the iron grade of the materials entering the furnace, greatly reduce the processing capacity of the subsequent mineral phase transformation–magnetic separation, and improve the production efficiency. In this study, based on the pre-selection results of previous research, it is decided to use a strong magnetic separation process to pre-enrich the low-grade refractory ferromanganese ores.

In the previous exploratory test, it was found that when the weak magnetic separation–strong magnetic pre-enrichment process is used to treat the raw ore, the yield of magnetic separation concentrate in the weak magnetic separation operation is ≤0.5%, so the single strong magnetic separation process is used to prepare the pre-enrichment concentrate in this pre-enrichment expansion test flow. And according to the results of the previous small test, it is determined to use 6500 Oe field strength to carry out a continuous test for the preparation of pre-enriched concentrate, and the results of the process inspection test are shown in Fig. 4. Fig. 4 shows that a pre-enriched concentrate with a yield of 84.77%, a TFe grade of 46.64% and a Mn grade of 16.94% can be obtained.

3.2 Mineral phase transformation of pre-enriched concentrates

3.2.1 Effect of roasting temperature. Roasting temperature is an important factor affecting the magnetization roasting effect.[25–28] To fully investigate the effect of roasting temperature on mineral phase transformation, different roasting temperatures were investigated under the conditions of a processing capacity of 80 kg h^{-1}, a N_2 dosage of 11.9 m^3 h^{-1}, a CO dosage of 8.7 m^3 h^{-1}, a H_2 dosage of 4.3 m^3 h^{-1}, and a magnetic field strength of 1520 Oe. The test results are shown in Fig. 5.

Fig. 5 reveals that with the increase in reduction temperature, the change in iron grade in the magnetic separation concentrate (iron concentrate) is not very obvious but fluctuates within the range of 66.50% to 67.85% with an average value of 67.10%. The iron recovery shows slight fluctuation, and the change is not obvious. The manganese grade in the magnetic separation tailings (manganese concentrate) does not change significantly with the increase in reduction temperature but fluctuates within the range of 51.21% to 53.61% with an average manganese grade of 42.81%. The manganese recovery increased slightly, and the manganese recovery varied within the range of 89.08% to 91.33%. Taken together, the roasting temperature of pre-enriched concentrate–mineral phase transformation should be controlled above 500 °C. Good indexes can be achieved, with iron concentrate grates greater than 66.5% and operational recovery above 94%, and manganese concentrate grades exceeding 51.2% and operational recovery greater than 89%.

3.2.2 Effect of reducing agent dosage. The reductants used in the mineral phase transformation are CO and H_2, and the amount of reductant has a significant effect on the reduction rate.[29–33] A low amount of reductant leads to an insufficient reaction, resulting in a low grade of roasted ore and a low recovery. On the contrary, an excessive amount of reductant will cause the over-reduction phenomenon and waste of reductant. In order to investigate the effect of reductant dosage on the phase transformation effect, the reductant dosage test was carried out under the condition of a reduction temperature above 500 °C, a dosage ratio of CO and H_2 of 2 : 1, a processing capacity of 80 kg h^{-1}, and a concentration of reductant of 45%. The test results are shown in Fig. 6.

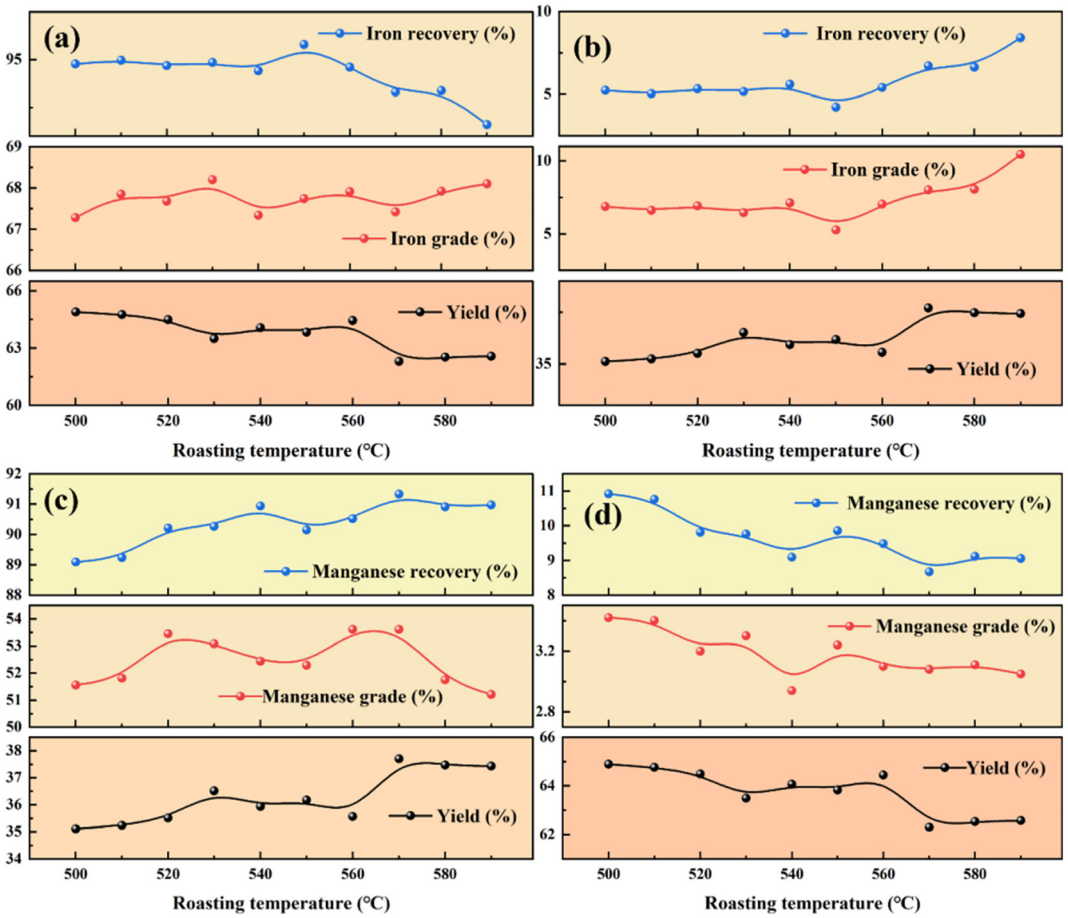

Fig. 5 Roasting temperature condition test: (a) grade, recovery, and yield of iron concentrate; (b) grade, recovery, and yield of iron tailings; (c) grade, recovery, and yield of manganese concentrate; (d) grade, recovery, and yield of manganese tailings.

Fig. 6 shows that with the increase in the total amount of reductant, the iron grade of the magnetic separation concentrate fluctuates between 67.07% and 68.08%, and it can be considered that the iron grade remains stable. The iron recovery also fluctuates less, varying from 95.23% to 93.18%. The manganese grade of magnetic separation tailings showed a trend of increasing and then decreasing. When the reductant dosage

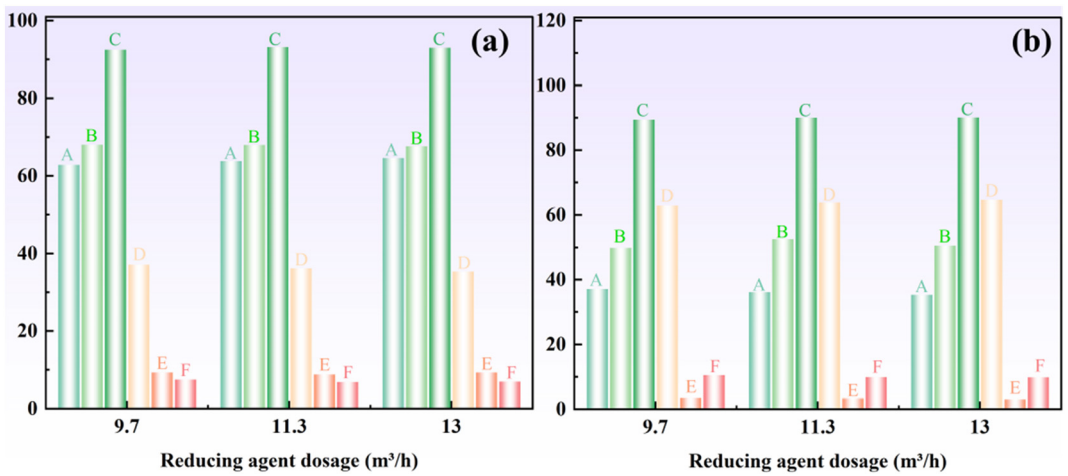

Fig. 6 Experimental conditions for reducing agent dosage: (a) iron concentrate yield A, grade B, and recovery C; iron tailings yield D, grade E, and recovery F; (b) manganese concentrate yield A, grade B, and recovery C; manganese tailings yield D, grade E, and recovery F.

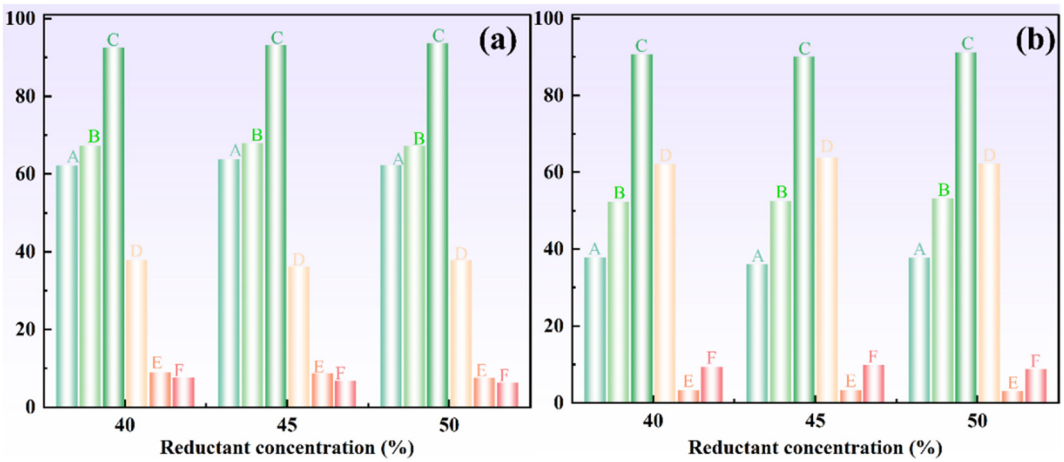

Fig. 7 Experimental conditions for reductant concentration: (a) iron concentrate yield A, grade B, and recovery C; iron tailings yield D, grade E, and recovery F; (b) manganese concentrate yield A, grade B, and recovery C; manganese tailings yield D, grade E, and recovery F.

increased from 9.0 m^3 h^{-1} to 11.3 m^3 h^{-1}, the manganese grade increased from 49.89% to 52.50%, and the manganese recovery showed a small increasing trend. Considering the above analysis, the suitable reductant dosage is 11.3 m^3 h^{-1}, which means that the excess coefficient of reductant is 1.4.

3.2.3 Effects of reducing atmospheres. In the test process, the gas mixture into the reactor contains non-reducing gas N_2. This part of the gas does not participate in the magnetization and reduction process of the material, but it occupies a certain amount of flow, thus increasing the flow rate of the material and shortening

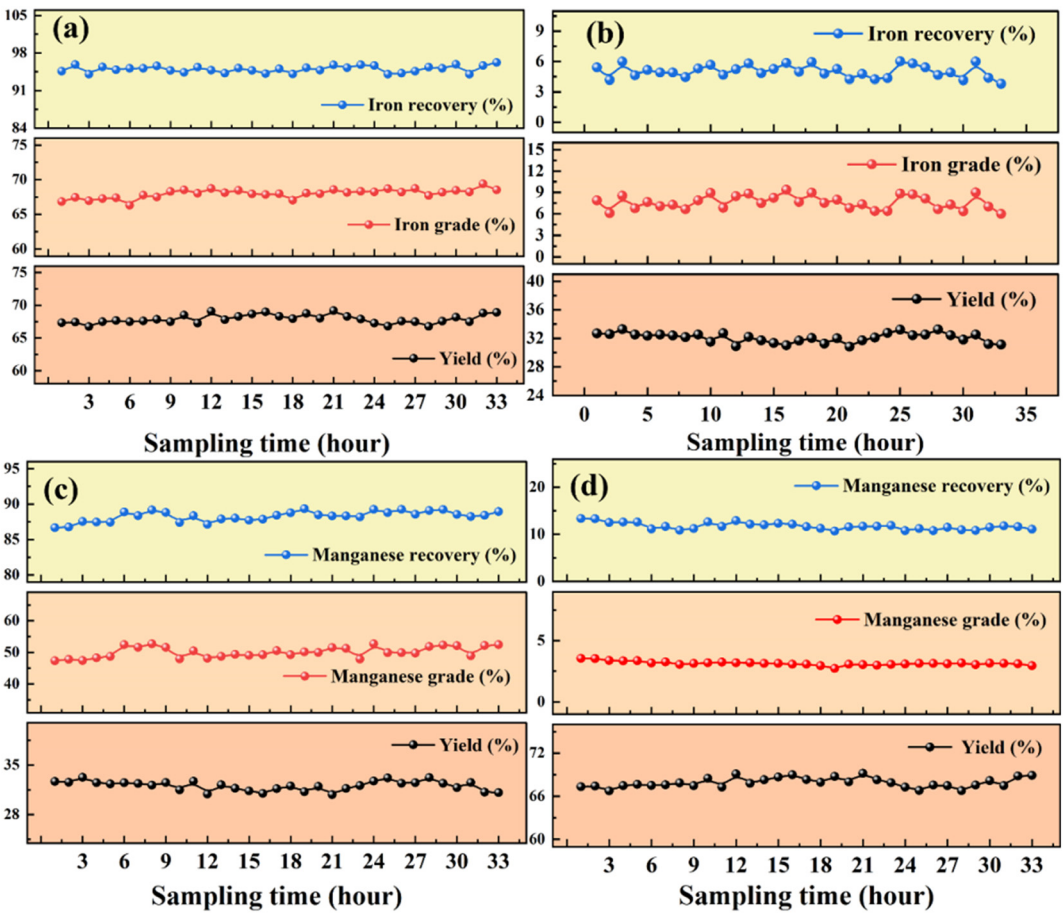

Fig. 8 Continuous stable operation test: (a) grade, recovery, and yield of iron concentrate; (b) grade, recovery, and yield of iron tailings; (c) grade, recovery, and yield of manganese concentrate; (d) grade, recovery, and yield of manganese tailings.

the residence time of the material in the reactor. Therefore, in the process of mineral phase transformation, it is very necessary to study the influence of the flow rate of N_2 in the gas mixture on the mineral phase transformation. The test was carried out at a processing capacity of 80 kg h^{-1}, a reductant CO and H_2 dosage ratio of 2:1, a total reductant dosage of 11.3 m^3 h^{-1}, and a reduction temperature of 500 °C. The results are shown in Fig. 7.

Fig. 7 demonstrates that as the reductant concentration increases, the iron grade of the magnetic separation concentrate increases and then decreases, and the iron recovery shows a small increasing trend. When the reductant concentration increased from 40% to 45%, the iron grade increased from 67.33% to 68.01%. When the reductant concentration continued to increase to 50%, the iron grade decreased to 67.18%. The manganese grade of the magnetic separation tailings varied between 52.40% and 53.31%, and the manganese recovery fluctuated within the range of 90.61% to 91.17%. Although the reductant concentration has some effect on the iron grade and iron recovery of iron concentrate and the manganese grade and manganese recovery of manganese concentrate, the effect is not obvious. In the whole range of test conditions, the iron concentrate grade was greater than 67%, and the iron recovery rate was greater than 92%; the manganese concentrate grade was greater than 52%, and the manganese recovery rate was greater than 9,0%. Considering the reduction effect, the suitable concentration of reductant was determined to be 45%.

3.3 Pre-enriched concentrate mineral phase transformation continuous stable operation test

Based on the results of the above tests, the operating conditions of the continuous phase transformation test were determined as follows: a processing capacity of 80 kg h^{-1}, a CO dosage of 7.5 m^3 h^{-1}, a aH_2 dosage of 3.8 m^3 h^{-1}, N_2 dosage of 13.8 m^3 h^{-1}, a reduction temperature of 500 °C, a total gas volume of 25.1 m^3 h^{-1}, and an excess coefficient of the reductant of 1.4. The continuous phase transformation test of the pre-enriched concentrates was carried out under these conditions to examine the smooth running of the suspension roaster and the stability of the

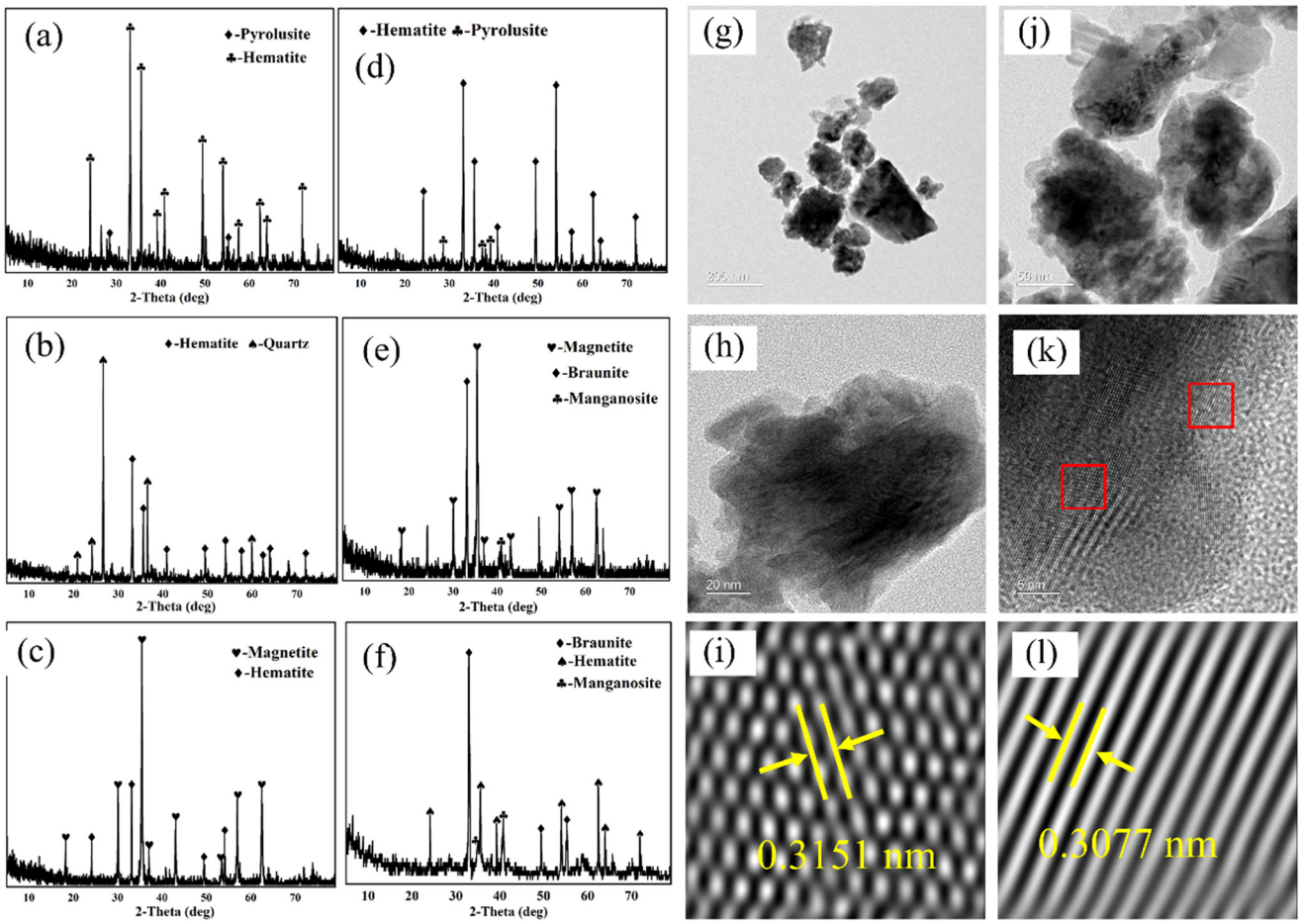

Fig. 9 Mineral phase transformation process: (a) XRD pattern of raw ore, (b) XRD pattern of strong magnetic concentrate, (c) XRD pattern of strong magnetic tailings, (d) XRD pattern of roasted ore, (e) XRD pattern of weak magnetic concentrate, (f) XRD pattern of weak magnetic tailings, (g)–(k) TEM analysis of roasted ore, (i) manganese lattice spacing, and (l) iron lattice spacing.

indicators. The suspension roaster operation and index stability were examined. Timing was initiated when the reactor temperature reached 500 °C. The stabilization test was conducted at 1 h intervals. During the stabilization test, small samples were taken every 1 h for 3 min, and the samples were sorted by magnetic separator tubes, and the beneficiation indexes were used as a standard to measure the stability of the continuous ore phase transformation process. The continuous stabilization test was carried out for a total of 20 h. The test results are shown in Fig. 8.

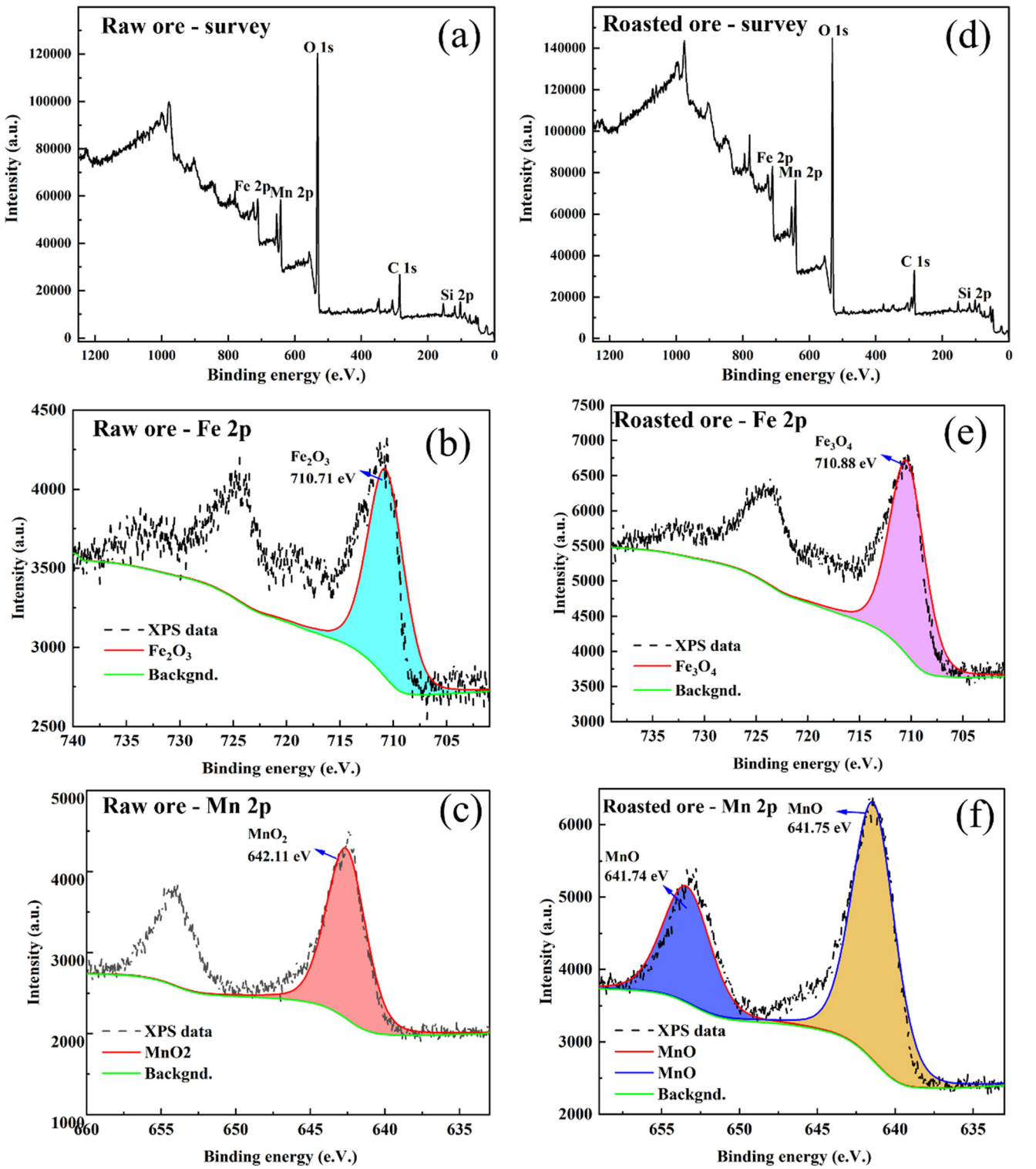

Fig. 10 XPS analysis test results of raw ore and roasted ore: (a)–(c) represent the XPS analysis images of the original ore; (d) XPS analysis graphs of roasted ore are shown in (e) and (f).

Fig. 8 declares that after magnetic separation of the sampled samples, the iron grades of iron concentrate were all above 66% with an average value of 67.97%. The iron recoveries were all greater than 93%, with an average value of 94.67%. The average value of the manganese grade of manganese concentrate was 49.85%, and the average value of manganese recovery was 88.24%. The above results show that the beneficiation indexes of the mineral phase transformation products are good and stable.

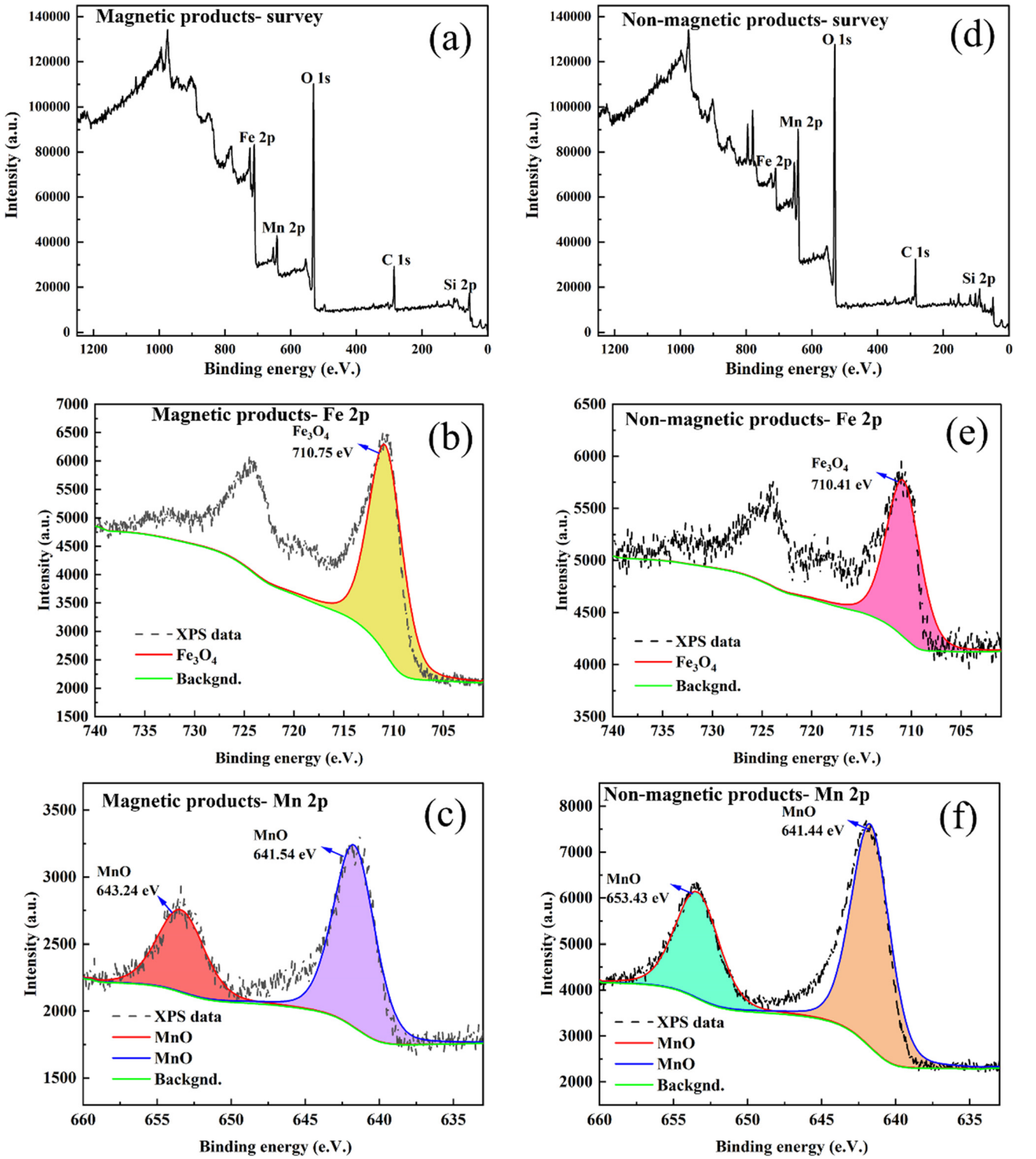

Fig. 11 XPS analysis test images of magnetic and non-magnetic products: (a)–(c) represent XPS analysis images of magnetic products; (d) XPS analysis graphs of non-magnetic products shown in (e) and (f).

3.4 Product analysis

To investigate the phase transformation and microstructure evolution of the main minerals in refractory ferromanganese ore during the mineral phase transformation process, XRD, HRTEM, XPS, and SEM–EDS were used to analyze the surface characteristics, microstructure, and crystal structure of the raw ore materials, pre-enriched products, mineral phase transformation products, and magnetic separation products, respectively. The results are shown in Fig. 9–12.

Fig. 9(a)–(f) shows that the main phases in the raw ore are hematite and pyrolusite. After pre-enrichment, hematite and pyrolusite were mainly enriched in the pre-enriched concentrate product, and quartz went into the pre-enriched tailings, thus realizing the casting off of impurities such as quartz. The mineral phase transformation products were mainly magnetite, manganosite, and braunite phases, indicating that after the mineral phase transformation process, hematite was transformed to magnetite, and pyrolusite was transformed into manganosite and braunite. After weak magnetic separation, magnetite was mainly enriched in the magnetic separation concentrate, and manganosite and braunite were mainly enriched in the magnetic separation tailings. The lattice streaks of iron minerals and manganese minerals in the mineral phase transformation products can be clearly observed as expressed in Fig. 9(g)–(l), and magnetite and manganosite show good crystallinity, and the spacing of the streaks is calculated to be d = 0.3077 nm and d = 0.3151 nm, respectively, and the corresponding crystal planes are {200} and {111}, respectively.

Fig. 10 reveals that the peaks of hematite and pyrolusite were found at binding energies of 710.71 eV and 642.11 eV, respectively, indicating that the main iron and manganese minerals in the raw ore were hematite and pyrolusite. The peaks of magnetite and manganosite were found at binding energies of 710.88 eV and 641.75 eV, respectively, indicating that magnetite and manganosite were the main iron and manganese minerals in the mineral phase transformation products. This process also indicates the transformation of hematite and pyrolusite to magnetite and manganosite, respectively, during the mineral phase transformation process. As can be seen from Fig. 11, the peaks of magnetite and manganosite were found in the magnetic separation concentrate at binding energies of 710.75 eV and 641.54 eV, respectively, but the diffraction peak intensities of magnetite were significantly stronger than those of

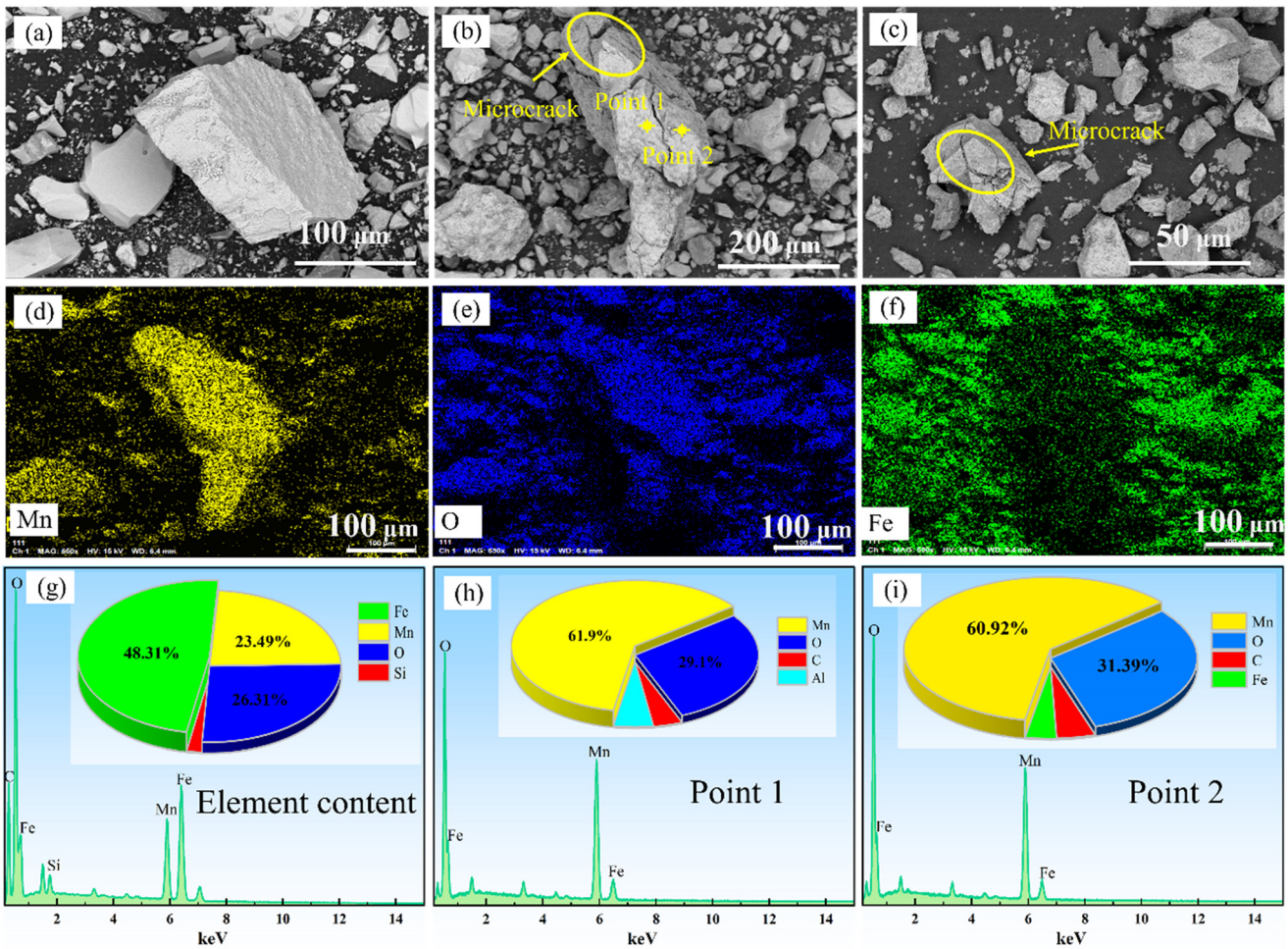

Fig. 12 SEM–EDS spectra of each product: (a) raw ore images; (b and c) pictures of roasted ore; (d–i) energy spectrum analysis of roasted ore.

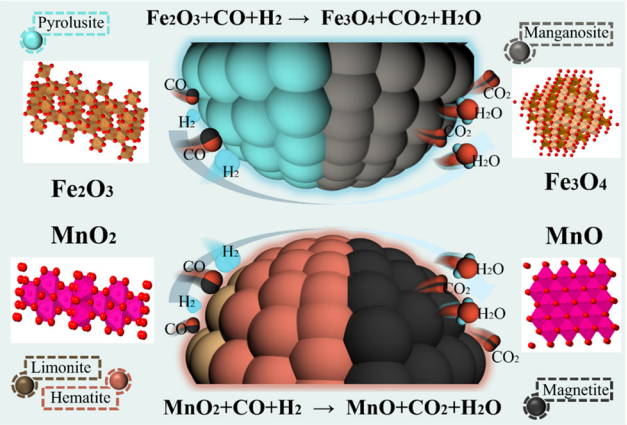

Fig. 13 The overall mechanism process.

manganosite, suggesting that the main mineral in the magnetic separation concentrate was magnetite. By magnetic separation, magnetite in the phase transformation products was separated and enriched in the magnetic separation concentrate. The peaks of magnetite and manganosite were found in the magnetic separation tailings at the binding energies of 710.41 eV and 641.44 eV, respectively, but the intensity of the diffraction peak of manganosite was significant for magnetite, indicating that the main mineral in the magnetic separation tailings was manganosite. Through magnetic separation, the manganosite in the mineral phase transformation products was separated and enriched in the magnetic separation tailings. Fig. 12 conveys that the surface texture of the raw ore is smooth and flat, and more loose and porous structures appear on the surface of the roasted products, indicating that the particles are transformed from a dense massive structure to a loose and porous massive structure through roasting. The overall mechanism process is shown in Fig. 13.

3.5 Introduction to industrial applications

Based on the above test conclusions, the team invented a complete set of equipment for the efficient utilization of mineral phase transformation of refractory ferromanganese ore resources and successfully researched and developed the world's first set of industrial technology of "pre-enrichment-mineral phase transformation-high-efficiency beneficiation" for refractory ferromanganese ore. The world's first 600 000 tons per year refractory ferromanganese ore pre-enrichment-mineral phase transformation-high-efficiency beneficiation project was built in Liaoning Sanhe Zambia Company. Excellent indexes are obtained: manganese concentrate with a manganese grade of 50.91% and a manganese recovery of 80.22%, and iron concentrate with an iron grade of 65.31% and an iron recovery of 93.13%. The recovery of manganese and iron increased by more than 20% compared with conventional technology, which is characterized by cleanliness, environmental protection, intelligence, and high efficiency.

4 Conclusions

(1) The grade of TFe in the raw ore sample of Zambian ferromanganese ore is 44.71%, and the grade of Mn is 17.86%. A pre-enriched concentrate with a grade of 46.64% TFe and 17.92% Mn can be obtained by using a section of a strong magnetic pre-enrichment process. For this pre-enriched concentrate, mineral phase transformation control tests, including the roasting temperature, reductant dosage, and reducing atmosphere, were carried out. The optimized process parameters are as follows: a reduction temperature above 500 °C, a processing capacity of 80 kg h^{-1}, a CO dosage of 7.5 m^3 h^{-1}, a H_2 dosage of 3.8 m^3 h^{-1}, a N_2 dosage 13.8 m^3 h^{-1}, a total gas volume of 25.1 m^3 h^{-1}, and a reductant excess coefficient of 1.4.

(2) The pre-enriched concentrate was continuously and stably operated at 500 °C. After magnetic separation, the average iron grade was 67.97% at an average recovery of 94.67% of iron concentrate, and the average manganese grade was 49.85% at an average recovery of 88.24% of manganese concentrate. The mineral phase transformation system in the continuous test process is characterized by good operation, stable control of working parameters, and excellent quality of roasted products. Mineral phase transformation technology is reliable and feasible in terms of equipment and technology.

(3) Through the mineral phase transformation technology, the precise control of mineral phase can be realized, and the pyrolusite and hematite have been transformed to manganosite and magnetite, respectively. Through magnetic separation, magnetite in the roasted ore was separated and enriched in the magnetic separation concentrate, and manganosite in the roasted ore was separated and enriched in the magnetic separation tailings.

Conflicts of interest

There are no conflicts to declare.

Data availability

The data supporting this article have been included as part of the supplementary information (SI). Supplementary information is available. See DOI: https://doi.org/10.1039/d5re00418g.

Acknowledgements

The authors would like to thank the National Key R&D Program Youth Scientist Project (Grant No. 2023YFC2909000) and China Postdoctoral Science Foundation (Grant No. 2024M751861).

References

1 M. Yellishetty and G. M. Mudd, Substance flow analysis of steel and long term sustainability of iron ore resources in Australia, Brazil, China and India, *J. Cleaner Prod.*, 2014, **84**, 400–410.

2 S. Yuan, R. Wang and P. Gao, *et al.* Suspension magnetization roasting on waste ferromanganese ore: A semi-industrial test for efficient recycling of value minerals, *Powder Technol.*, 2022, **396**, 80–91.

3 S. K. Tripathy, M. K. Mallick and V. Singh, *et al.* Preliminary studies on teeter bed separator for separation of manganese fines, *Powder Technol.*, 2013, **239**, 284–289.

4 S. B. Kumar, S. T. Kumar and Y. M. Rama, *et al.* Influence of mineralogy on the dry magnetic separation of ferruginous manganese ore-A Comparative Study, *Minerals*, 2021, 11.

5 J. Lan, Y. Sun and Y. Du, *et al.* Environmentally-friendly bioleaching of manganese from pyrolusite: Performance and mechanisms, *J. Cleaner Prod.*, 2020, **249**, 119354.

6 X. Wang, Y. Xie and K. Chen, *et al.* Bioleaching assisted conversion of refractory low-grade ferruginous rhodochrosite to Mn-Fe based catalysts for sulfathiazole degradation, *Chem. Eng. J.*, 2022, **427**, 130804.

7 C. J. Niyonzima, L. Luo and E. E. Edo, *et al.* Mineralogical Characterization and Optimization of Fe and Mn Through Roast-Leaching of Ferromanganese Ore, *Min. Metall. Explor.*, 2021, **38**(3), 1–15.

8 V. Singh, K. V. K. Reddy, S. K. Tripathy, P. Kumari, A. K. Dubey, R. Mohanty, R. R. Satpathy and S. Mukherjee, A sustainable reduction roasting technology to upgrade the ferruginous manganese ores, *J. Cleaner Prod.*, 2021, **284**, 124784.

9 D. Zhu, J. Xu, Z. Guo, J. Pan, S. Li, L. Pan and C. Yang, Synergetic utilization of copper slag and ferruginous manganese ore via co-reduction followed by magnetic separation process, *J. Cleaner Prod.*, 2020, **250**, 119462.

10 A. Cheraghi, H. Becker, H. Eftekhari, H. Yoozbashizadeh and J. Safarian, Characterization and calcination behavior of a low-grade manganese ore, *Mater. Today Commun.*, 2020, **25**(101382), 2352–4928.

11 N. Peng, Q. Pan, H. Liu, Z. Yang and G. Wang, Recovery of iron and manganese from iron-bearing manganese residues by multi-step roasting and magnetic separation, *Miner. Eng.*, 2018, **126**, 177–183.

12 S. K. Tripathy, M. K. Mallick, V. Singh and Y. Rama Murthy, Preliminary studies on teeter bed separator for separation of manganese fines, *Powder Technol.*, 2013, **239**, 284–289.

13 Z. Zhang, Q. Liu and J. Ran, Experimental Study on Mineral Processing of Iron Manganese Ore in Xinjiang, *Miner. Prot. Util.*, 2014(2), 26–29, (in Chinese).

14 Z. You, G. Li, Y. Zhang, Z. Peng and T. Jiang, Extraction of manganese from iron rich MnO_2 ores via selective sulfation roasting with SO_2 followed by water leaching, *Hydrometallurgy*, 2015, **156**, 225–231.

15 X. Wang, Y. Xie, K. Chen, L. Yi, Y. Wang and Y. Zhang, Bioleaching assisted conversion of refractory low-grade ferruginous rhodochrosite to Mn-Fe based catalysts for sulfathiazole degradation, *Chem. Eng. J.*, 2022, **2022**(427), 130804.

16 G. Wen, S. Yuan and Z. Dong, *et al.* Mechanism and process study of spent lithium iron phosphate batteries by medium-temperature oxidation roasting strategy, *Sep. Purif. Technol.*, 2025, **356**, 129987.

17 G. Wen, S. Yuan and Z. Dong, *et al.* Recycling of spent lithium iron phosphate battery cathode materials: A review, *J. Cleaner Prod.*, 2024, **474**, 143625.

18 Q. Zhang, Y. Sun and Y. Qin, *et al.* Siderite pyrolysis in suspension roasting: An in-situ study on kinetics, phase transformation, and productproperties, *J. Cent. South Univ.*, 2022, **29**(6), 1749–1760.

19 S. Yuan, W. Zhou and Y. Han, *et al.* Efficient enrichment of low-grade refractory rhodochrosite by preconcentration-neutral suspension roasting-magnetic separation process, *Powder Technol.*, 2020, **361**, 529–539.

20 S. Yuan, W. Zhou and Y. Han, *et al.* Selective enrichment of iron particles from complex refractory hematite-goethite ore by coal-based reduction and magnetic separation, *Powder Technol.*, 2020, **367**, 305–316.

21 S. Yuan, W. Zhou and Y. Han, *et al.* Individual enrichment of manganese and iron from complex refractory ferromanganese ore by suspension magnetization roasting and magnetic separation, *Powder Technol.*, 2020, **373**, 689–701.

22 S. Yuan, W. Zhou and Y. Han, *et al.* Separation of manganese and iron for low-grade ferromanganese ore via fluidization magnetization roasting and magnetic separation technology, *Miner. Eng.*, 2020, **152**, 106359.

23 W.-T. Zhou, Y.-X. Han and Y.-S. Sun, *et al.* Strengthening iron enrichment and dephosphorization of high-phosphorus oolitic hematite using high-temperature pretreatment, *Int. J. Miner., Metall. Mater.*, 2020, **4**, 443–453.

24 W. Zhou, Y. Sun and Y. Han, *et al.* An innovative technology for utilization of oolitic hematite via microwave fluidization roasting: phase, structure and reaction kinetics analyses, *Miner. Process. Extr. Metall. Rev.*, 2022, **43**(6), 757–770.

25 N. S. Sahu, P. Behera and S. Sahoo, *et al.* A Critical Review on the Magnetization Roasting of Low/Lean-Grade Iron Ore Resources Using Renewable/Non-Renewable Reductant: An Approach Towards Iron ore Sustainability, *J. Sustain. Metall.*, 2025, **11**(1), 1–26.

26 X. Cui, X. Ning and J. Zhang, *et al.* Insights into sulfur migration and transformation during the magnetization roasting of iron tailings and textile dyeing sludge, *Waste Manage.*, 2025, 19181–19188.

27 A. Abdalla, R. S. Mohanty and S. Yadav, *et al.* Assessment of Zero Waste Approach by Enhancing Chromium-to-Iron Ratio in Chromite Ore Through Magnetizing Roasting: A Novel Comparative Sustainable Study of Conventional and Hybrid Microwave Heating Methods, *J. Sustain. Metall.*, 2024, **10**(4), 1–19.

28 S. Zhang, T. Zhou and C. Li, *et al.* Research progress and prospect of fluidized bed metallic ore roasting technology: A review, *Fuel*, 2024, **378**, 132717.

29 X. Yuan, T. Jiang and Y. C. Tay, *et al.* Magnetization roasting combined with multi-stage extraction for selective recovery of lithium from spent lithium-ion batteries, *Sep. Purif. Technol.*, 2024, **338**, 126349.
30 L. Xiao, Z. Wentao and G. Xiangai, Thermal analysis and isothermal reduction kinetics of alkaline hematite in an advanced suspension roaster, *Sep. Purif. Technol.*, 2023, **323**, 124493.
31 C. Jie, L. Hongyi and H. Dong, *et al.* Magnesiation roasting kinetics exploration of vanadium slag toward minimization of tailing toxicity, *J. Hazard. Mater.*, 2023, **452**, 131378.
32 S. N. Sahu, B. C. Meikap and S. K. Biswal, Reduction in fossil fuel consumption by exploiting separation of refractory grade oolitic iron ores using black plum leaf litter via magnetization roasting & pelletization; a small step toward decarbonization & sustainability, *Sep. Purif. Technol.*, 2023, **311**, 123327.
33 Y. Shuai, X. Hanxin and W. Ruofeng, *et al.* Improved iron recovery from low-grade iron ore by efficient suspension magnetization roasting and magnetic separation, *Miner. Eng.*, 2022, **186**, 107761.